Geophysical Journal International

Geophys. J. Int. (2015) **200,** 1281–1285 doi: 10.1093/gji/ggu469
GJI Seismology

EXPRESS LETTER

Fluid pressure waves trigger earthquakes

Francesco Mulargia[1] and Andrea Bizzarri[2]

[1]*Dipartimento di Fisica e Astronomia, Settore di Geofisica, Università di Bologna, Italy. E-mail: francesco.mulargia@unibo.it*
[2]*Istituto Nazionale di Geofisica e Vulcanologia, Sezione di Bologna, Bologna, Italy*

Accepted 2014 December 3. Received 2014 December 3; in original form 2014 October 10

SUMMARY

Fluids—essentially meteoric water—are present everywhere in the Earth's crust, occasionally also with pressures higher than hydrostatic due to the tectonic strain imposed on impermeable undrained layers, to the impoundment of artificial lakes or to the forced injections required by oil and gas exploration and production. Experimental evidence suggests that such fluids flow along preferred paths of high diffusivity, provided by rock joints and faults. Studying the coupled poroelastic problem, we find that such flow is ruled by a nonlinear partial differential equation amenable to a Barenblatt-type solution, implying that it takes place in form of solitary pressure waves propagating at a velocity which decreases with time as $v \propto t^{[1/(n-1)-1]}$ with $n \gtrsim 7$. According to Tresca-Von Mises criterion, these waves appear to play a major role in earthquake triggering, being also capable to account for aftershock delay without any further assumption. The measure of stress and fluid pressure *inside* active faults may therefore provide direct information about fault potential instability.

Key words: Elasticity and anelasticity; Fracture and flow; Friction; Earthquake interaction, forecasting and prediction.

INTRODUCTION

The initiation of seismic rupture is generally called *triggering* due to the wide difference between the tiny energy required for activation and the huge energy that comes then into play.

The experimental phenomenology yields that:

(i) Spatial localization applies; earthquakes occur on pre-existent spatially defined regions of mechanical weakness, that is, the *faults*.

(ii) Time invariance applies; since the timescale of earthquake recurrence on the same fault segment is 100–1000 yr, while the timescale of the driving stress is a geological process 3–4 order of magnitudes slower, earthquakes can be taken as time invariant.

(iii) Friction coefficients are very low; static friction on fault zones is much lower than in bulk (undamaged) rock, and in the laboratory: it has values $\mu < 0.3$ rather than 0.7–1, because impermeable gouge zones reduce sliding friction by trapping pore fluids at pressures which, under strain, are higher than hydrostatic (Rice 1992). More explicitly, we can assume that the range $\mu \leq 0.3$ is representative of an intermediate stage of a fluid-permeated fault; due to thermal pressurization of pore fluids, in the very early stage of the slip motion, that is after a slow slip off the order of 10^{-3} m, the effective normal stress is reduced (see, e.g. Mulargia & Geller 2003; Mulargia *et al.* 2004; Bizzarri & Cocco 2006), so that the resulting effective friction coefficient at the onset of the macroscopic slip is much lower than typical Byerlees values $\mu \sim 0.7$. Indeed, the issue of a low static friction coefficient at the onset of earthquake slip is *per se* a matter of high interest, and is the object of a separate study, currently in preparation. Suffice here to say that our assumption of a static friction coefficient of the order of 0.3 (or less) is corroborated by very consistent field evidence (Zoback *et al.* 1987; Raesenberg & Simpson 1992; Iio 1997; Yamamoto & Yabe 2001; Yamamoto *et al.* 2002; Kubo & Fukuyama 2004).

(iv) Triggering stresses are very low; triggering has been experimentally measured at stresses $\sigma \geq 10^{-2}$ MPa (Stein 1999), achieving statistical significance over $\sim 3 \times 10^4$ event samples at $\sigma \geq 10^{-2}$ MPa (Vidale *et al.* 1998).

(v) Triggering occurs preferentially—but not only—on the most favourably oriented faults; these, oriented in the principal axes system σ^{I}, σ^{II}, σ^{III} on the plane $n_i x_i$, with $n_i = [\pm\sqrt{(2)}/2, 0, \pm\sqrt{(2)}/2]$.

(vi) Triggering extends to considerable distances; earthquakes are triggered by other events or by fluid injection at distances up to 10–10^2 km (Stein 1999; Parsons 2002).

(vii) Triggering is a generally delayed process; aftershocks and reservoir induced earthquakes occur with delay times from hours up to 10–20 yr (Parsons 2002).

The fundamental equation to describe the above appears to be the Tresca–Von Mises criterion, prescribing that rupture occurs when the effective stress σ^{eff} is larger than the critical stress σ_R (Terzaghi *et al.* 1996)

$$\sigma^{\mathrm{eff}} > \sigma_R, \qquad (1)$$

where

$$\sigma^{\mathrm{eff}} = \sigma_{\mathrm{shear}} + \mu\left(\frac{\sigma^{\mathrm{I}}+\sigma^{\mathrm{III}}}{2} - p_{\mathrm{fluid}}\right) \tag{2}$$

with p_{fluid} standing for the pore fluid pressure. The deviatoric stress values on faults can be inferred from the earthquake stress drop as follows. While the experimental *in situ* static friction coefficients are very small, the dynamic friction coefficients are bound to be even smaller (Mulargia *et al.* 2004; Bizzarri 2011), that is $\mu \to 0$, implying that earthquakes release virtually all deviatoric stresses. Indeed, there is plenty of evidence, both from laboratory experiments and from theoretical and numerical models, that many different physical and chemical mechanisms can lead to very low dynamic stresses, which in turn eventually lead to a nearly complete stress release; readers can refer to Bizzarri (2014; sections 8.3–8.6 and 9.2.1) and references cited therein. Hence, we postulate that the maximum shear stress on faults is equal to the stress drop, which is 1–10 MPa, independent of earthquake size and depth (Kanamori & Anderson 1975)

$$1\,\mathrm{MPa} \le s_{ij} = \sigma_{ij} - \frac{\sigma_{kk}}{3}\delta_{ij} \le 10\,\mathrm{MPa}. \tag{3}$$

By releasing all crustal strain both seismically and aseismically, the faults keep deviatoric stresses in the crust low. In fact, the *in situ* measurements made all over the world (Zoback & Healy 1984) yield that the stresses in the crust are modest perturbations to a lithostatic condition, $\sigma_{ij} = \delta_{ij}\sigma_{\mathrm{vert}} \sim 27\,\mathrm{MPa\,km^{-1}}$, with deviatoric stresses about at most a third of this value.

Comparing these with the stresses on faults, the ones that drive earthquakes—that is 1–10 MPa irrespective of earthquake magnitude and focal depth—yields that faults reside in an almost exactly lithostatic stress state, except for minute occasional perturbations, of order o^4 or less (i.e. of relative amplitude $\le 10^{-4}$), that destroy a delicate equilibrium and lead to earthquakes. Note how this is in full agreement with the criticality paradigm (Rundle 1988; Corral 2004).

Let us now consider in detail how occasional tiny perturbations trigger earthquakes.

AFTERSHOCKS: THE MOST OBVIOUS CASE OF EARTHQUAKE TRIGGERING

The most prominent evidence of earthquake triggering is represented by aftershocks: each sizeable earthquake is followed by a large number of other nearby earthquakes, usually smaller in size. Aftershocks are best defined statistically as an increase in the local seismicity rate. The latter has a surge following the 'main shock' and slowly returns to its background level after several years, following Omori's law

$$N = \frac{1}{(c+t)^P}, \tag{4}$$

where N is the number of events per unit time, c a constant and $P \sim 1$.

Stress redistribution, sometimes called the 'Coulomb stress', is classically assumed at the basis of aftershock triggering (Stein 1999). However, approximately only 60 per cent of the observed aftershocks are correlated with a (calculated and geodetically supported) stress increase, while 40 per cent are related to a stress decrease (Parsons 2002). Yet, this is *not* the major problem with a Coulomb stress aftershock origin. Being an elastic effect, Coulomb stress transient propagates at the velocity of seismic (surface) waves, $v \sim 1$–$3\,\mathrm{km\,s^{-1}}$, similar to that of the 'main shock' rupture velocity, extending the latter to all domains in which stress redistribution allows to satisfy eqs (1) and (2). Hence, more than triggering, the Coulomb stress is likely to rule the propagation of the 'main shock' itself and, in a cascade effect, its size. Even the inclusion of 'rate and state' constitutive laws allows it to justify delays of the order of 10 s (Stein 1999; Bizzarri 2011), accounting for some very early aftershocks, but leaving all the others unexplained. Therefore, only the assumption of either afterslip or a viscoelastic crust can reconcile Coulomb approach with experiment (Perfettini & Avouac 2007), but this would in turn imply a high correlation with time-dependent crustal strains which is not apparent from the dense surface and space based geodetic networks.

We show here that a completely different mechanisms may drive aftershock triggering and, possibly, the initiation of most earthquakes.

FLUID PRESSURE WAVES AS EARTHQUAKE STARTERS

The stress and pore pressure changes induced in the crust by a pressure change at a given 'injection' point can be calculated using the coupled equations of deformation and flow. These, under the approximation of plane strain, can be written as (Biot 1956)

$$\omega\nabla^2\left[\sigma_{xx} + \sigma_{zz} + \frac{3}{B(1+\nu_u)}p_{\mathrm{fluid}}\right] = \frac{\partial}{\partial t}\left[\sigma_{xx} + \sigma_{zz} + \frac{3}{B(1+\nu_u)}p_{\mathrm{fluid}}\right], \tag{5}$$

where ω is the hydraulic diffusivity, B is the Skempton co-efficient and ν_u the undrained Poisson co-efficient. In a 2-D domain, sufficient to deal with most problems, the coupled solution converges to the decoupled one (Roeloffs 1988)

$$\omega\nabla^2\left[\frac{3}{B(1+\nu_u)}p_{\mathrm{fluid}}\right] = \frac{\partial}{\partial t}\left[\sigma_{xx} + \sigma_{zz} + \frac{3}{B(1+\nu_u)}p_{\mathrm{fluid}}\right] \tag{6}$$

which approximates the coupled stress field with the elastic stress field and evaluates separately the diffusion contribution.

Since fluid pressure diffuses essentially along narrow drained paths (fractures and joints) with high hydraulic diffusivity (Talwani *et al.* 2007; Liu *et al.* 2011; Xue *et al.* 2013) rather than through the bulk pores, we can further restrict the problem to one dimension.

A solution of this equation which has proven to adequately explain earthquake triggering by artificial reservoir impoundment (Talwani *et al.* 2007) can be written as

$$p(r,t) = \gamma p_0\,\mathrm{erf}\left(\frac{r}{\sqrt{4\omega t}}\right) + p_0\,\mathrm{erfc}\left(\frac{r}{\sqrt{4\omega t}}\right), \tag{7}$$

where r is the distance from the injection point, γ is an non-dimensional constant representing the relative weight of elastic versus diffusion terms, erf and erfc are, respectively, the error function and the complementary error function, and p_0 is the input pressure at the source. Given the linearity of the problem, a solution for a given time history of the input pressure $P(t)$ at the injection point can be obtained from eq. (7) by the principle of superposition.

While knowing the existence and the geometry of the drained path beforehand is impossible, only assuming its existence, that is the predominance of the diffusion terms at $t \sim 0$, allowed a satisfactory fit to the experimental data on triggered earthquakes (Talwani *et al.* 2007; Liu *et al.* 2011). This assumption is also supported by the evidence that hydraulic diffusivity of crustal rocks varies experimentally in the laboratory and in the field over 16 decades, but its effective value in the cases of triggered seismicity

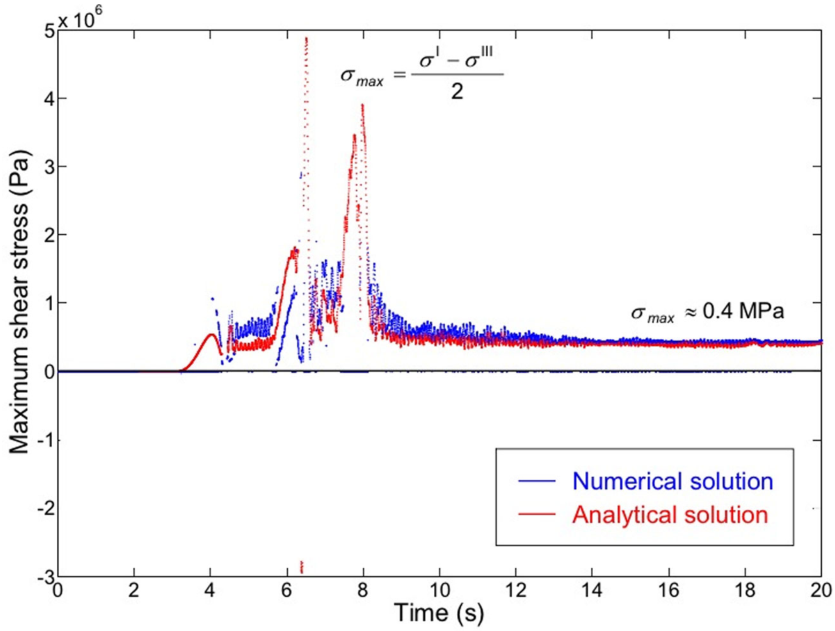

Figure 1. Time history of the maximum shear stress $\frac{\sigma^{I}-\sigma^{III}}{2}$ produced by a source with seismic moment 3.66×10^{19} Nm (moment magnitude $M_W \sim 7.0$), on a receiver sited at the hypocentral depth (7.3 km) and at 10 km off the fault plane (i.e. at a distance of 18 km from the hypocentre). The elastic parameters of the medium are: $v_p = 6$ km s^{-1}, $v_s = 3.464$ km s^{-1} and $\rho = 2670$ kg m^{-3}. At each time step the eigenvalues σ^{I} and σ^{III}, $\sigma^{I} \geq \sigma^{III}$, are computed both numerically (blue curve) and analytically from Cardano's solution (red curve).

ranges only over two decades, from 0.1 to 10 m^2 s^{-1}. Note how the drained paths, that is the patterns of high porosity, are not the effect of fluid overpressures, but rather the vehicle for their propagation (*cf.* Screaton & Ge 2000).

To analyse a typical case of earthquake triggering, we model the elastic and pore fluid contributions in eq. (6) as follows. For the elastic contribution, we consider the elastic waves produced by a double-couple point source approximating a vertical strike-slip fault, and solve the elasto-dynamic problem numerically as in Bizzarri (2011). The solution for the time evolution of the maximum shear stress at a target receiver is shown in Fig. 1. As a typical behaviour, we find a strong transient simultaneous to the arrival of seismic waves, followed by a static component one order of magnitude smaller, representing the residual stress change—either an increase or a decrease—imposed by the earthquake. It is worth recalling that the amplitude of the stress peaks, as well as that of the residual stresses, are directly linked to the strain released by the earthquake, that is to its magnitude (Kanamori & Anderson 1975; Bizzarri 2011). For example, at the same receiver on which a M_W 5.0 earthquake imposes a residual stress of 2 KPa, a M_W 8.0 earthquake imposes 6.6 MPa.

The pore fluid pressure contribution of eq. (6) relates to the classic problem of the 'porous medium' non-linear partial differential equations (Zwillinger 1997) of type

$$\frac{\partial c}{\partial t} = \mathrm{div}(c^n \,\mathrm{grad}\, c), \quad n > 0,$$

which deal with generalized diffusion. They apply to a variety of diffusion problems, ranging from the diffusion of gases and fluids in porous media to the pressure pulse propagation of a nuclear detonation (Barenblatt 1952). A solution can be effectively written using self-similarity as (Barenblatt 1952; Lacey *et al.* 1982)

$$p(r,t) = \left[\frac{n}{2(n+2)}\right]^{1/n} t^{-1/(n+2)} \left[a^2 - x^2 t^{-2/(2+n)}\right]^{1/n}, \qquad (8)$$

where a is a positive constant which depends on n and is related to the total energy of the process. This solution describes a pressure pulse propagating at a finite velocity $v \propto t^{[1/(n-1)-1]}$, at odds with the equation of heat diffusion, which predicts an infinite propagation velocity, except for the relativistic constraints. On the contrary, here a finite propagation velocity is built in the solution. Using measured values of parameters (Talwani *et al.* 2007), that is $\gamma \simeq 0.01$–0.001 and $\omega \simeq 10$–30, gives that fluid pressure (normalized to input pressure) propagates as a wave. Its peak (marked with an arrow in Fig. 2) occurs always well after the input pressure decrease has begun, that is with a substantial time delay.

The example of Fig. 2 mimics the sudden pressure pulse produced by an earthquake in the draining path provided by the fault system. We assume that the slip on the fault crushes the solid matrix around the slip zone, so that by stress continuity the fluid pressure is raised from hydrostatic to lithostatic—that is by $\sim$17 MPa km^{-1} (170 MPa at a focal depth of 10 km)—in the slip time, that is $\sim$10 s. The fluid pressure remains constant for 10–10^2 s, as long as the fluid does not begin flowing in the drained pattern. A power law decay of the input pressure has been assumed to guarantee an Omori-like decay of the diffusion term in eq. (4). The peak pressure propagates at a velocity slowly decreasing with time, in agreement with eq. (8) provided that $n \gtrsim 7$. The power law nature of this equation implies a fluid propagation velocity of a few kilometres per day after a few days and a few kilometres per year after a few years (*cf.* Mulargia & Bizzarri 2014). Note how, while the fluid injection overpressure is independent of the 'main shock' size, the latter is tied to dimension of the source region (Kanamori & Anderson 1975), and therefore of the areal extension of the injection sources. Larger main shocks inject fluids over larger areas, leading to trigger larger events for the same argument, reversed.

Diffused pressure values a few per cent of the input are commonly attained. These values are only apparently small, since the hydrostatic pore fluid pressure at hypocentral depths is 3 orders of magnitude larger than the stresses which have been found to

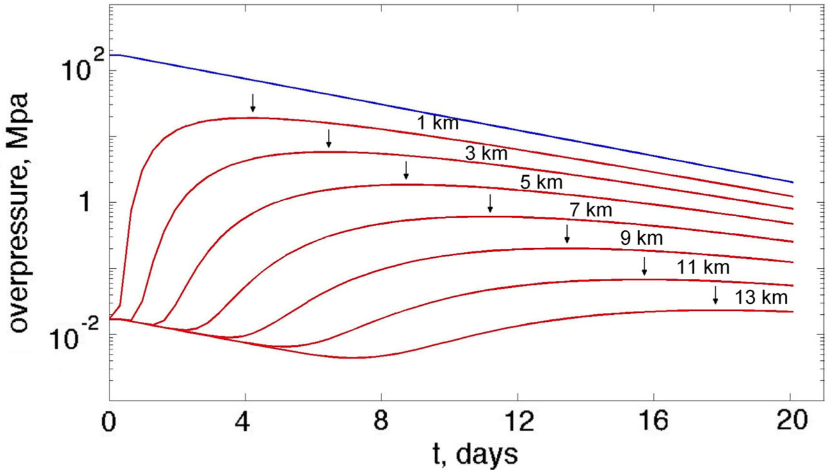

Figure 2. The input fluid pressure (blue curve) and the fluid pressure waves at different distances from the injection point (red curves). Arrows indicate the local maxima. A load function decrease compatible with an Omori decay was assumed together with parameter values compatible with reservoir induced seismicity (see text), that is a relative weight of elastic versus pressure diffusion $\gamma = 0.01$, and a hydraulic diffusivity $\omega = 10\ \mathrm{m}^2\ \mathrm{s}^{-1}$; a variation of these parameters within, respectively, more than one order of magnitude and a factor of 5, produced no essential change.

trigger earthquakes near reservoirs. Hence, the fluid pressure waves appear as a leading mechanism for triggering earthquakes, be them naturally produced by nearby earthquakes or by the anthropogenic injection of pressurized fluids in the subsoil.

As apparent from Fig. 2, which illustrates the fluid pressure as a function of time at different distances from the source, the solution is generally a solitary wave, since it is spatially localized and has negligible negative amplitude. However, its shape is not time invariant and, due to the principle of superposition, it does not possess any particle-like interaction property; therefore it is *not* a soliton. Comparing Fig. 1 to Fig. 2, it is evident that fluid pressure waves act at much slower time scales than the Coulomb stress. Moreover, it emerges that the static perturbation due to the Coulomb stress is significantly lower than that due to fluid pressure.

CONCLUSIONS

The elastic and diffusion terms of eq. (6) appear to rule the process of earthquake initiation with their widely different velocities and time constants: the elastic (Coulomb stress), ruling rupture propagation and determining the size of each event, and the diffusion term, determining the delayed triggering of other events. Indeed, earthquake triggering comprises both terms: the diffusion of a pulse pressure wave starts the process on the spatial domain reached by the draining path, and the subsequent Coulomb stress redistribution propagates the rupture to the final event size. This mechanism, supported by the phenomenology of the seismic events triggered by reservoir impoundment, appears as a basic mechanism for earthquake initiation, and its the role can be confirmed by measuring fluid pressure *inside* faults. The process we suggest frames earthquake initiation in a different perspective, potentially defining new measurable patterns prior to occurrence, even if not necessarily reflecting in the level of surface water wells. At the same time, the injection of pressurized fluids in the subsoil—as is practice in oil and gas production—should be effected with great care to avoid anthropogenic earthquake triggering (Mulargia & Bizzarri 2014).

ACKNOWLEDGEMENTS

This work was performed with an RFO grant of the Università di Bologna.

REFERENCES

Barenblatt, G.I., 1952. On some unsteady motions of a liquid or a gas in a porous medium, *Prikl. Math. i. Mekh.,* **16,** 67–78 (in Russian).

Biot, M.A., 1956. General solutions of the equationsof elasticity and consolidation for a porous material, *J. Appl. Mech.,* **23,** 91–96.

Bizzarri, A., 2011. On the deterministic description of earthquakes, *Rev. Geophys.,* **49,** RG3002, doi:10.1029/2011RG000356.

Bizzarri, A., 2014. The mechanics of seismic faulting: recent advances and open issues, *La Rivista del Nuovo Cimento,* **37**(4), 181–271.

Bizzarri, A. & Cocco, M., 2006. A thermal pressurization model for the spontaneous dynamic rupture propagation on a three-dimensional fault: 2. Traction evolution and dynamic parameters, *J. geophys. Res.,* **111,** B05304, doi:10.1029/2005JB003864.

Corral, A., 2004. Long-term clustering, scaling, and universality in the temporal occurrence of earthquakes, *Phys. Rev. Lett.,* **92,** 108501, doi:10.1103/PhysRevLett.92.108501.

Iio, Y., 1997. Frictional coefficient on faults in a seismogenicregion inferred from earthquake mechanism solutions, *J. geophys. Res.,* **102,** 5403–5412.

Kanamori, H. & Anderson, D.L., 1975. Theoretical basis of some empirical relations in seismology, *Bull. seism. Soc. Am.,* **65,** 1073–1095.

Kubo, A. & Fukuyama, E., 2004. Stress fields and fault reactivation angles of the 2000 western Tottori aftershocks and the 2001 northern Hyogo swarm in southwest Japan, *Tectonophysics,* **378,** 223–239.

Lacey, A.A., Ockendon, J.R. & Tayler, A.B., 1982. 'Waiting time' solutions of a nonlinear diffusion equation, *SIAM J. Appl. Math.,* **42,** 1252–1264.

Liu, S., Xu, L. & Talwani, P., 2011. Reservoir induced seismicity in the Dajangkou Reservoir: a quantitative analysis, *Geophys. J. Int.,* **185,** 514–526.

Mulargia, F. & Bizzarri, A., 2014. Anthropogenic triggering of large earthquakes, *Nature Sci. Rep.,* **4,** 6100, doi:10.1038/srep06100.

Mulargia, F. & Geller, R.J., 2003. *Earthquake Physics and Seismic Risk Reduction,* Kluwer, 338 pp.

Mulargia, F., Castellaro, S. & Ciccotti, M., 2004. Earthquakes as three stage processes, *Geophys. J. Int.,* **158,** 98–108.

Parsons, T., 2002. Global Omori law decay of triggered earthquakes: large aftershocks outside the classical aftershock zone, *J. geophys. Res.,* **107,** B02199, doi:10.1029/2001JB000646.

Perfettini, H. & Avouac, J.P., 2007. Modeling afterslip and aftershocks following the 1992 Landers earthquake, *J. geophys. Res,* **112,** B07409, doi:10.1029/2006JB004399.

Raesenberg, P.A. & Simpson, R.W., 1992. Response of regional seismicity to the stati stress change produced in the Loma Prieta earthquake, *Science,* **255,** 1687–1690.

Rice, J.R., 1992. Fault stress states, pore pressure distributions, and the weakness of the San Andreas Fault, in *Fault Mechanics and Transport Properties of Rocks*, pp. 475–504, eds Evans, B. & Wong, T.-F., Academic Press.

Roeloffs, E.A., 1988. Fault stability changes induced beneath a reservoir with cyclic variations in water level, *J. geophys. Res.,* **83,** 2107–2124.

Rundle, J.B., 1988. A physical model for earthquakes, 1. Fluctuations and interactions, *J. geophys. Res.,* **93,** 6237–6254.

Screaton, E. & Ge, S., 2000. Anomalously high porosities in the proto-decollement zone of the Barbados accretionary complex: do they indicate overpressures?, *Geophys. Res. Lett.,* **27,** 1993–1996.

Stein, R.S., 1999. The role of stress transfer in earthquake occurrence, *Nature,* **402,** 605–609.

Talwani, P., Chen, L. & Gahalaut, K., 2007. Seismogenic permeability, k_s, *J. geophys. Res.,* **112,** B07309, doi:10.1029/2006JB004665.

Terzaghi, K., Peck, R.B. & Mesri, G., 1996. *Soil Mechanics in Engineering Practice,* 3rd edn, John Wiley, 592 pp.

Vidale, J., Agnew, D., Oppenheimer, D., Rodriquez, C. & Houston, H., 1998. A weak correlation between earthquakes and extensional normal stress and stress rate from lunar tides., *EOS, Trans. Am. geophys. Un. (suppl.),* **79,** F641.

Xue, L. *et al.*, 2013. Continuous permeability measurements record healing inside the Wenchuan Earthquake Fault Zone, *Science,* **340,** 1555–1559.

Yamamoto, K. & Yabe, Y., 2001. Stresses at sites close to the Nojima Fault measured from core samples, *Island Arc,* **10,** 266–281.

Yamamoto, K., Sato, N. & Yabe, Y., 2002. Elastic property of damaged zone inferred from in-situ stresses and its role on the shear strength of faults, *Earth Planets Space,* **54,** 1181–1194.

Zoback, M.D. & Healy, J.H., 1984. Friction, faulting, and 'in situ' stresses, *Ann. Geophys.,* **2,** 689–698.

Zoback, M.D. *et al.*, 1987. New evidence of the state of stress of the San Andreas fault system, *Science,* **238,** 1105–1111.

Zwillinger, D., 1997. Handbook of Differential Equations, *Library of the Congress,* Academic Press, 757 pp.